Exploring potential energy surfaces around valley-ridge inflection points

Wolfgang Quapp[1*], Grace Hsiao-Han Chuang[2] and Josep Maria Bofill[3,4]

[1*]Mathematisches Institut, Universität Leipzig, Augustus-Platz PF 100920, Leipzig, D-04009, Germany, Orcid: 0000-0002-0366-1408.
[2] Physics of Complex Systems, Max Planck Institute, Noethnitzer Str. 38, Dresden, D-01187, Germany, Orcid: 0000-0003-0145-9596.
[3]Química Inorgànica i Orgànica, Secció de Química Orgànica, Universitat de Barcelona, Martí i Franquès 1, Barcelona, 08028, Catalunya, Spain, Orcid: 0000-0002-0974-4618.
[4]Institut de Química Teòrica i Computacional (IQTCUB), Universitat de Barcelona, Martí i Franquès 1, Barcelona, 08028, Catalunya, Spain.

*Corresponding author(s). E-mail(s): quapp@math.uni-leipzig.de;
Contributing authors: hhchuang@pks.mpg.de; jmbofill@ub.edu;

Abstract

Purpose: Valley-ridge inflection (VRI) points play an important role in organic chemistry, especially in post-TS bifurcations. We explain a new discovery of a special structure of the region with another type of VRI point.
Methods: We apply the theory of Newton trajectories (NTs) and gradient extremals (GEs) to cases of two dimensional potential energy surfaces.
Results: We have found a case where the VRI of a new type is traversed by a quasi-regular NT, a semi-singular one, so to speak. Here, the gradient is the eigenvector to zero eigenvalue.
Conclusion: The new type of VRI point is connected with a 'dead' valley of the PES. The example is a nice demonstration that the index theorem for NTs holds, nevertheless. NTs and GEs are important tools to explore the region of a VRI point.

25-3-2025

Keywords: Potential energy surface, Transition state, Valley-ridge inflection point, Regular and singular Newton trajectory, Gradient extremal

1 Introduction

Bifurcations are omnipresent in natural sciences [1, 2], including valleys on a potential energy surface (PES). They are a long studied subject [3–8]. The bifurcation can take place before the transition state (TS) of a dissociation [9, 10], as it is demonstrated by an internal vibrational redistribution [11]. It also can happen at the TS [12, 13]. Or in contrast, the study of organic chemical reactions shows often bifurcations after the first TS. The theoretical understanding of the underlying mechanisms that govern selectivity, i.e. product distributions is of central interest [14–19]. And finally, the bifurcation can coalesce with a TS [6, 20]. Bifurcations can also take place in radiationless deactivation of organic dyes on the lower PES [21].

Understanding in particular asymmetric post-transition state bifurcations is essential for predicting reaction selectivity in complex chemical systems [22, 23]. Of course, here the reaction pathways inherently require at least a two-dimensional (2D) description, as long as a pathway over a single transition state bifurcates into two distinct product pathways. The PES has two consecutive saddles of index 1 with no intervening energy minimum. Between the two index-1 saddles, one of which has higher energy than the other, there must be a valley ridge inflection (VRI) point [6, 24–28].

The reaction is initiated when a trajectory crosses the area of the higher saddle (forming the entrance channel) and may approache the lower energy saddle. On either side of the lower energy saddle, there are two minimum wells. The question of interest is which well does the trajectory enter (predicting the product selectivity)? It could leave the standard intrinsic reaction path, the IRC [29–32].

One can assume that the VRI plays a role in selectivity. Certainly the VRI is a geometrical feature of the PES. Two conditions are fulfilled there: The curvature of the PES is zero, which implies that the Hessian matrix has a zero eigenvalue, and the gradient of the potential is perpendicular to the eigenvector corresponding to the zero eigenvalue. This means that the landscape of the PES in the neighborhood of the VRI changes its shape from a valley to a ridge which gave the region the name VRI.

In synthetic chemistry, identifying the key functional groups that influence reaction pathways is crucial for designing efficient synthesis strategies, especially when dealing with large molecules containing multiple functional groups. If the dominant degrees of freedom are known, especially the VRI region, chemists can target these features to streamline synthesis.

In the next Section we repeat the definition of the reaction path models of interest: Newton trajectories (NTs) and gradient extremals (GEs). In Section III we discuss different relations of a VRI region to the singular NT traversing it, for different 2D test PES. In Section VI we add a discussion. A conclusion is given in Section V.

2 Models of the reaction path

This work concerns a mathematical excursion which discusses the use of NTs for the exploration of a special PES, $V(\mathbf{x})$ given in reference [33], and in particular its VRI points. An NT is a curve $\mathbf{x}(t)$ where the gradient, $\mathbf{g}$, of the PES is parallel to a given direction, $\mathbf{f}$, at every point

$$\mathbf{g}(\mathbf{x}(t)) \quad || \quad \mathbf{f} \ , \tag{1}$$

t is a curve length parameter. Curves that solve Eq.(1) are of particular interest in mechanochemistry, where the direction $\mathbf{f}$ is the direction of an external force [34–36]. A possibility to follow a curve fulfilling this property (1) is the definition of a projector matrix. If $\mathbf{r} = \mathbf{f}/|\mathbf{f}|$ is the normalized direction then

$$\mathbf{P} = (\mathbf{I} - \mathbf{r}\mathbf{r}^{\mathbf{T}})$$

projects on direction $\mathbf{r}$. Eq.(1) looks then

$$\mathbf{P}\,\mathbf{g}(\mathbf{x}(\mathbf{t})) = \mathbf{0}\ .$$

Its derivation can be used to develop a predictor-corrector method [6].

Alternatively, the approach of Eq.(1) was formulated in a differential equation by Branin [6, 37, 38]

$$\frac{d\mathbf{x}(t)}{dt} = \pm Det(\mathbf{H}(\mathbf{x}(\mathbf{t})))\ \mathbf{H}^{-\mathbf{1}}(\mathbf{x}(\mathbf{t}))\,\mathbf{g}(\mathbf{x}(\mathbf{t}))\ , \tag{2}$$

$\mathbf{H}$ is the Hessian of the second derivatives of the PES. It is important that the matrix

$$\mathbf{A}\ = \mathbf{Det}(\mathbf{H})\ \mathbf{H}^{-\mathbf{1}} \tag{3}$$

is desingularized when the Hessian becomes singular. It is called the adjoint matrix for $\mathbf{H}$. The full Hessian matrix can be computationally expensive at each step of the positions $\mathbf{x}(t)$. However, it can be updated [39–41]. A first numerical step starts from a stationary point in direction $\mathbf{f}$. The following steps then ensure that the gradient maintains this direction [6]. The plus + sign in Eq.(2) is used for an NT from a minimum to an SP of index one, but the minus - vice versa. If the energy increases monotonically along an NT then it can serve for a reaction path variable.

Note that NTs have the nice property that they connect stationary points with an index difference of one [6, 38, 42], compare appendix 1. The index here counts the number of negative eigenvalues of the Hessian matrix at the stationary point. If we start at a minimum with index zero, we obtain a next saddle point (SP) with index one. A special case is a singular NT that crosses a valley ridge inflection (VRI) point [6]. The characterization of the VRI is the zero point of the right hand side of the Branin equation (2)

$$\mathbf{A}\,\mathbf{g} = \mathbf{0} \tag{4}$$

but where the gradient is not zero, $\mathbf{g}(\mathbf{x}) \neq \mathbf{0}$. A singular NT has four branches through the VRI point. It typically connects a minimum with a saddle of index two and two SPs of index one via the VRI. A VRI represents the branching of a valley into two valleys and an intermediate ridge, or complementarily, the branching of a ridge into two ridges and a valley in between. Mathematically, the Hessian has a zero eigenvector orthogonal to the gradient [6, 31, 43–45]. With these properties, we can fully investigate any 2D toy PES such as the one in this work, as well as any high-dimensional PES. We can follow a one-dimensional curve by Eq. (2) in any dimension. For a PES with more than two dimensions manifolds of VRI points arise

[46, 47]. There is an illustrative introduction to the higher dimensional case [48]. The following of an NT is included in the COLUMBUS program system [49] (under the name reduced gradient following, RGF). There are some links to different programs [50, 51]. If the PES is symmetric, the VRI manifold often forms a symmetry hypersurface. However, asymmetric VRI manifolds can also be computed [46, 50, 52, 53]. Recently, the role of VRI points in dynamical processes has been discussed [54]. The Newton trajectory method has been established in chemistry since 1998, see refs. [36, 55–60] and further references therein. We report that NTs are calculated for medium molecules with up to dimension 486 [61].

A second kind of curves which also can serve for the description of reaction valleys are gradient extremals (GE) [6, 62–65] where holds

$$\mathbf{H}(\mathbf{x}(t))\mathbf{g}(\mathbf{x}(t)) = \lambda\ \mathbf{g}(\mathbf{x}(t)) \tag{5}$$

thus on a GE the gradient, $\mathbf{g}$, is an eigenvector of the Hessian, $\mathbf{H}$, with (varying) eigenvalue λ. GEs are represented in the following figures by black dashed curves. A VRI point is crossed by a GE if the pseudoconvexity index μ [66, 67] changes its sign

$$\mu = \frac{\mathbf{g}^T\,\mathbf{A}\,\mathbf{g}}{\mathbf{g}^T\,\mathbf{g}}\ . \tag{6}$$

Below we explain a new type of a VRI region by GEs. However, the condition (6) does not apply. Note that special GEs can fit the valley branching problem by the determination of a GE bifurcation itself [63, 64]. Typically, N GEs emanate from a stationary point, if N is the dimension of the PES. Then the GE to the smallest eigenvalue λ_{min} describes the baseline of the reaction valley. This GE can be considered a static representation of a reaction path.

Another interesting type of curves is the boundary between regions of a different index of the Hessian of the PES. For the case of 2D surfaces $V(x,\,y)$ they are given by

$$Det(\mathbf{H}) = V_{xx}\ V_{yy} - V_{xy}^2 \quad = \quad 0 \tag{7}$$

and they are represented by thin green curves in the following figures.

3 2D example PES

A series of PES is used of Ref.[33]

$$V(x,y) = x^4 - 2x^2 + y^4 + y^2 - 1.5x^2y^2 + x^2y - c\,y^3 \tag{8}$$

as shown in the following figures. The constant c is a parameter that varies here between 1 and 2.

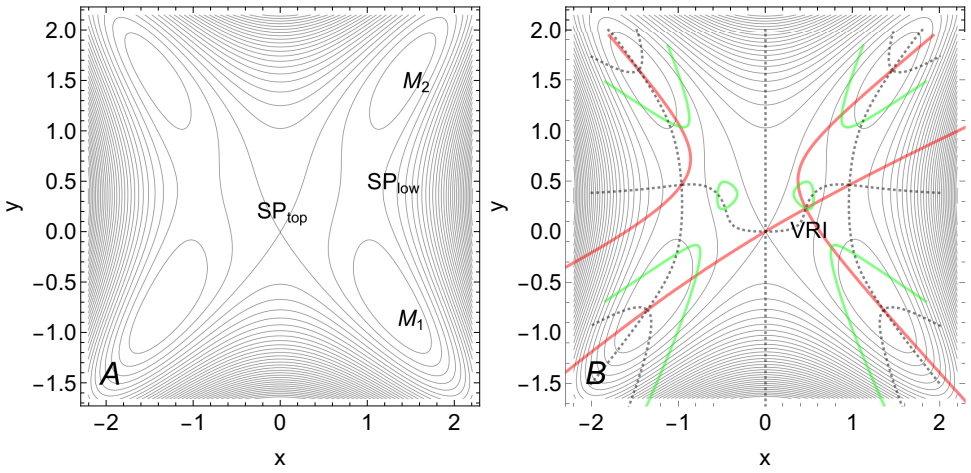

Fig. 1 **A:** Level lines of PES (8) for c=1.5. The axis x=0 is an axis of symmetry. M_1 is a minimum, SP_{low} is the transition state to the minimum M_2. The global SP_{top} lies central on the y axis at point $(0,0)$. **B:** A VRI point is located between SP*top* and the stationary points in the valley on the right hand side. Three types of curves are shown: Bold red is the singular NT through the right VRI point, GE curves are dashed black, and the Det(**H**)=0-lines are thin green.

3.1 PES for c=1.5

First we discuss a 'normal' case for parameter c=1.5 of PES (8). One can observe in Fig.1 that the right valley from M_1 to M_2 bifurcates to the SP_{top}. There are only stationary points of index zero, minima, and of index one, transition states (TS). By different curves we can determine the exact VRI point. This is demonstrated in Fig.1B. Here the 4 branches of the singular red NT intersect at the VRI. The search direction of the singular NT is $\mathbf{f}_{red}$=(-1.3, 0.33). It is the gradient at the solution of Eq.(4). The VRI is at (x, y)=(0.4627, 0.229) with

$$\mathbf{g} = \begin{pmatrix} -1.3155 \\ 0.3371 \end{pmatrix}, \quad \mathbf{H} = \begin{pmatrix} -1.13 & 0.29 \\ 0.29 & -0.07 \end{pmatrix} \text{ and } \mathbf{A} = \begin{pmatrix} -0.07 & -0.29 \\ -0.29 & -1.13 \end{pmatrix}.$$

The vector with Eq.(4) is $\mathbf{A}\,\mathbf{g} = \mathbf{0}$ thus the gradient is the zero eigenvector of $\mathbf{A}$, and the second eigenvalue is $\lambda = -1.204$ being the eigenvalue of the matrix $\mathbf{H}$ for the eigenvector $\mathbf{g}$. The vector

$$\mathbf{v} = \begin{pmatrix} 0.3371 \\ 1.3155 \end{pmatrix}$$

is then the zero eigenvector of the Hessian orthogonally to the gradient. It is the characteristic of the VRI point. Note that Hessian and adjoint Hessian have the same eigenvectors, but for the eigenvalues λ_i of the Hessian and μ_i of the adjoint the following applies for every i [68, 69]

$$\mu_i\ \lambda_i \ = \ Det(\mathbf{H}) \ = \ \prod_{k=1}^{N} \lambda_k \ . \tag{9}$$

For $N = 2$ it means $\mu_1 = \lambda_2, \quad \mu_2 = \lambda_1$.

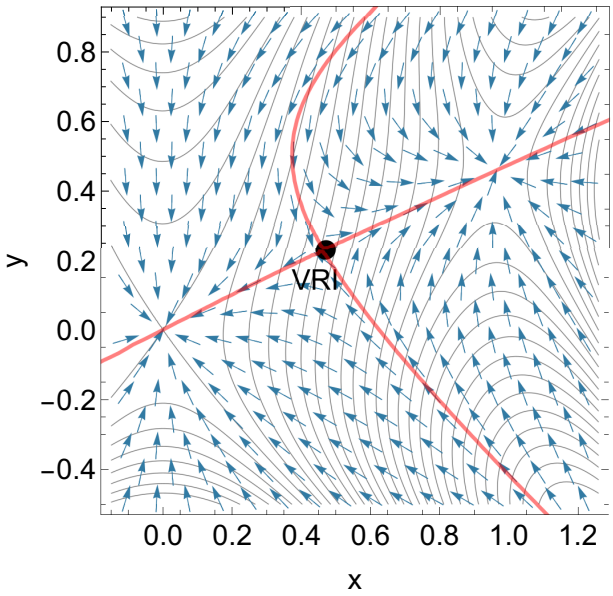

Fig. 2 Vector field of the Branin Eq.(2) with plus sign on a section of the PES of Fig. 1. The VRI point is characterized by the hyperbolic touching of the corresponding regular NTs.

A thin green border line of Det(**H**) crosses a GE there. Thus, all three curves cross at the VRI point. (The calculation of these curves is described in an appendix.) The boundaries of the different Det(**H**) regions are given by the condition of Eq.(7). Normally they are curvilinear, so that the points of a molecule on a higher dimensional PES with $Det(\mathbf{H}) = \mathbf{0}$ form curved hypersurfaces.

The VRI is intersected by its own singular NT which is represented by the bold red lines. The four branches form an almost orthogonal cross at the VRI point. We name VRI of type S this long known type of a VRI point. Singular NTs are the boundaries of families of NTs that connect the minimums, M_i, to different SPs. Any two neighboring branches of the singular NT form a corridor for all NTs connecting a given minimum, M, with the same SPi [70]. The stationary points are also crossed by the NT and by the various branches of the GEs.

In Fig.2, the vector field of the right hand side of the Branin Eq.(2) is included on the PES with c=1.5. The hyperbolic touching of the corresponding NTs before and after the VRI point is a characterization of this region.

3.2 PES for c=1

A 3D representation of this PES is shown in Fig.3. Here we develop the bizarre case of interest for a 'half' singular NT. One can observe in Fig.4 that the right valley from M_1=M uphill to the right hand side bifurcates again to a valley to the $SP_{top} = SP$, the only SP which remains. There is also a thin green border line, as well as a GE which crosses it. We take this crossing for the VRI point of a new type. However, there is no bifurcating NT through this VRI point. In contrast, we find a fairly regular NT connection the SP with the minimum M over this VRI point. It is

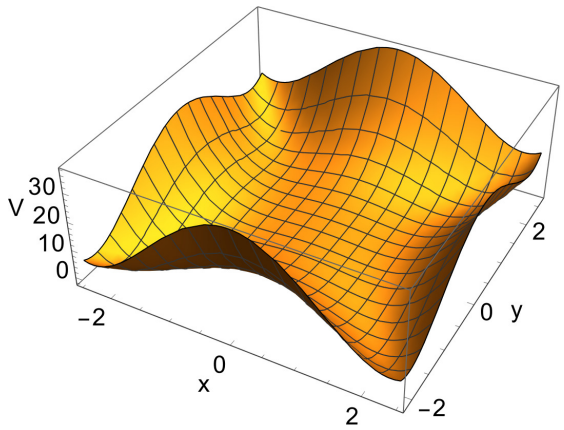

Fig. 3 3D representation of PES (8) for c=1. Only two uphill valleys remain. There are still two minima at the bottom, and the central SP also remains.

at (x, y)=$(0.5562, 0.2972)$ with

$$\mathbf{g} = \begin{pmatrix} -1.3533 \\ 0.468 \end{pmatrix}, \quad \mathbf{H} = \begin{pmatrix} 0.04 & 0.13 \\ 0.13 & 0.35 \end{pmatrix} \text{ and } \mathbf{A} = \begin{pmatrix} 0.35 & -0.13 \\ -0.13 & 0.04 \end{pmatrix}.$$

The search direction of the 'half'-singular NT is $\mathbf{g}$=$\mathbf{f}_{red}$=(-1.3533, 0.468). The Hessian matrix has the zero eigenvector being the gradient, and

$$\mathbf{A}\,\mathbf{g} = \begin{pmatrix} -0.5282 \\ 0.1827 \end{pmatrix} = 0.39\ \mathbf{g} \neq \begin{pmatrix} 0 \\ 0 \end{pmatrix}. \tag{10}$$

A zero eigenvector of the Hessian is retained by the gradient, in this case. But 0.39 is the second eigenvalue of the direction orthogonal to the gradient. The value of the Branin vector is not zero which really shows that there is no 'normal' VRI point of type S from the point of view of NTs. This is also an indication that such rare cases cannot be determined by the VRI finding method using the condition $\mathbf{A}\,\mathbf{g}$=$\mathbf{0}$ [52, 53]. Additionally, also μ of definition (6) does not change its sign, thus it does not indicate the VRI point. Nevertheless the GE crosses the line Det($\mathbf{H}$)=0 and has there the special eigenvalue $\lambda = 0$. We name this VRI point of type G for its crossing only by a GE. No bifurcation of a reaction trajectory takes place here. The condition $\mathbf{H}\,\mathbf{g} = \mathbf{0}$, at the other hand, is the criterion for an optimal barrier breakdown point (oBBP) in mechanochemistry [34–36]. But that is again another story.

With the blue NT in Fig.4 A we add a regular NT beginning at minimum M and initially following the valley uphill. It shows a turning point (TP) high in the PES mountains where the energy reaches a maximum, and it returns as a regular connection to the only remaining SP at point $(0, 0)$. Its search direction is $\mathbf{f}_{blue}$=(-0.53, 1.11). The blue NT is an indication of the reason why this special VRI point is useless for chemistry: The valley at the right hand side is a 'dead' valley without a further TS and minimum. There cannot be a stable chemical structure. On the right sight of the

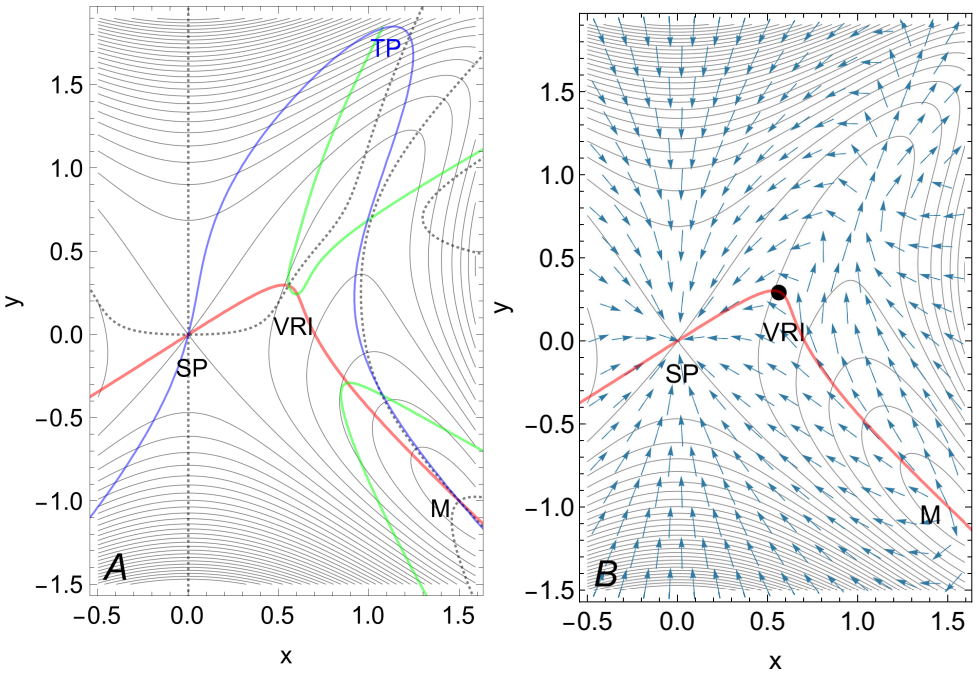

Fig. 4 **A:** Three kinds of curves are drawn on the PES for c=1. Red is the remainder of the singular NT through the right VRI point of type G, black dashed are the GE curves, and green are the Det(**H**)=0-lines. The blue curve is an ordinary regular NT. **B:** Vector field of Branin Eq.(2). The VRI point is embedded in a nice flow of regular NTs.

PES only one minimum and one SP exist. Every NT starting in the right minimum has to find its way to the central SP. There are no other stationary points, so the NT through the VRI point must also be 'regular'. There is no target for it to bifurcate to. The entire right half-plane is one reaction channel [70]. The VRI point exists but the index theorem acts that the VRI does not disturb the channel of regular NTs.

In Fig.4 B the vector field of the right hand side of the Branin Eq.(2) is again included. The NTs flow around the VRI point in an unusual way. Their hyperbolic contact at the VRI point is lost.

3.3 Action of the index theorem for singular NTs

Index Theorem for NTs
Regular NTs connect stationary points with an index difference of one [6, 38, 42]. This will be violated by a singular NT.
Proof: see appendix 1.

Fig.5A represents a quasi shoulder region of the former SP_{low} and the former minimum M_2 for parameter $c = 1.125$. The two branches of the singular NT to SP_{low} and to the minimum M_2 come close together. They form quasi parallel branches. After the two stationary points they continue and end in a TP. The four branches intersect

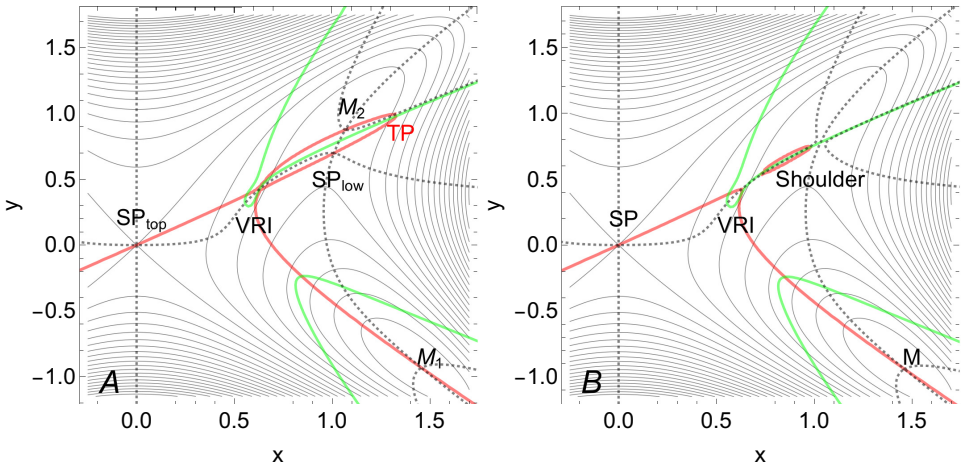

Fig. 5 **A:** PES (8) for c=1.125. The former low SP and the former minimum M_2 nearly merge and almost form a flat shoulder. The minimum M_1 is still at the bottom, and the central SP also remains. **B:** PES for c=1.11 which forms a PES with a shoulder point. Red is the rest of the singular NT through the right VRI point, black dashed are GE curves, and green are the Det(**H**)=0-lines.

at a small angle at the VRI point. However, the index theorem also applies here in its usual form. Stationary points are connected by regular NTs (not shown) and the singular NT connects with two branches the two SPs of index one, and with two other branches the two minima with index 0.

The situation changes further in panel B of Fig.5 where we obtain a real shoulder point. Here the former SP_{low} and the former minimum M_2 have merged. The remaining point is a stationary point with a zero gradient and a zero eigenvector along the valley line. The PES is obtained by parameter $c = 1.11$. The shoulder is demonstrated by the GEs there, which do not cross as in stationary points but avoid a crossing near the former SP_{low}. Three branches of the singular NT remain from the VRI. It is the limiting case. The next step is then the case of Fig.4 with c=1, where the character of the singular NT is lost, and where the connection to the former shoulder region also is finally lost.

For comparison, we include still two neighboring NTs to the singular one, in Fig.6, in blue color. The dashed NT follows the search direction (-1, 0.36), it bypasses the VRI region on the right. The pure blue NT follows the (-1, 0.3) direction and runs to the SP at the left hand side of the VRI.

4 Discussion

An important model for a reaction coordinate in chemistry is the steepest descent from SP, the intrinsic reaction coordinate (IRC) [29, 30]. In case of a symmetric PES and a totally symmetric axis through the SP [71–73], the IRC can cross a possible VRI point on this downhill path [31, 74–76]. However, on an asymmetric PES, the VRI is usually not located on the steepest descent from the SP [9, 77, 78]. There, any other reaction

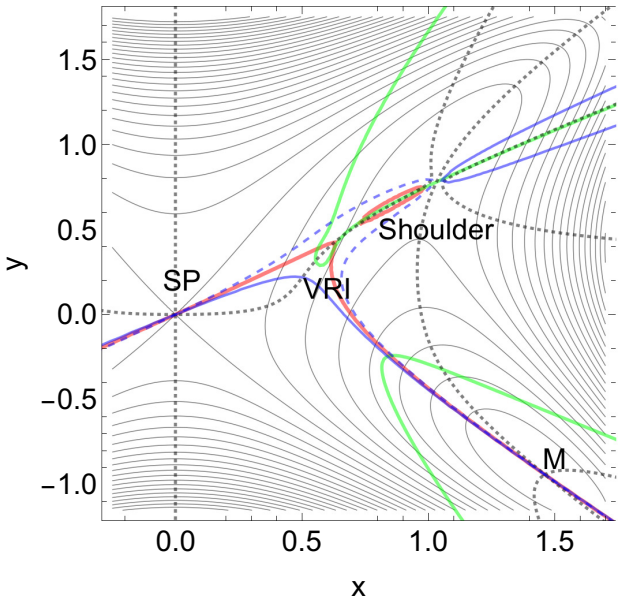

Fig. 6 Two regular NTs in blue are additionally included in Fig.5 B, see text.

trajectory could bifurcate off from the IRC [79]. It is incorrect that the IRC splits itself at the VRI point [80, 81]. The IRC can split only at stationary points, where the gradient is zero, and where different directions for the further travel downhill can open. SPs are the singular points of the steepest descent trajectories. Analogous to NTs near VRI points, these trajectories follow hyperbolic curves around SPs.

One way out is a dynamical approach by many trajectories over the entrance SP region [19, 82–89]. This method contrasts with static models of a reaction pathway for IRC, NT, or GE. Localization through two sets of dynamical trajectories bifurcating near the VRI point is one way of a certain determination of the VRI point and product selectivity. Although dynamic trajectories can theoretically identify the VRI, this approach is unrealistic and hardly feasible in a real system. According to the ergodic hypothesis [90], a single trajectory could explore the entire configuration space if it moves forever in phase space, including the VRI. However, this is a multidimensional problem, and the growth of dimensions is proportional to the number of atoms involved. Finding a specific outcome amidst such complexity is highly unrealistic.

The other possibility is the calculation of GEs and a singular NT to precisely locate the VRI. Of course, this exceptional VRI point of case $c = 1$ of Fig.4 cannot be detected using dynamical trajectories or a singular NT. One can speculate that such exceptional VRI points also exist on other, older known PES. Because 'dead' valleys often exist. For example the well known Müller-Brown PES [91] has such a valley on the left hand side, and no singular NT crosses it [68, 69]. In contrast, here also crosses a GE the Det($\mathbf{H}$)=0-line at point (x, y)=(-1.09771, 0.6487) and the Hessian indeed has a zero eigenvalue where the eigenvector is the gradient, compare Fig. 7.

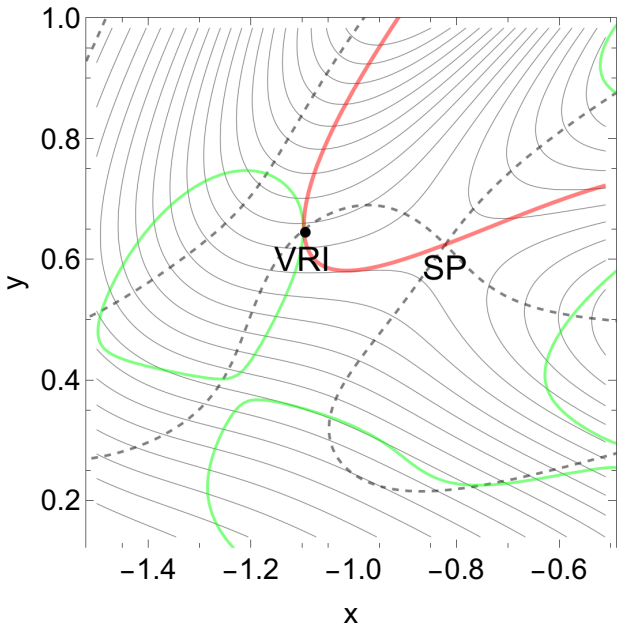

Fig. 7 MB surface with proposed VRI of type G at the branching of the left global valley.

5 Conclusion

We use Newton trajectories (NT), gradient extremals (GE) and Det(**H**)=0-lines of the PES to explore the region of a VRI point. Long known are VRI points of type S where a singular NT bifurcates. Its side branches form static models of a reaction path bifurcation. They can serve for models of trajectories to two different products.

By changing the parameter c of the PES of Ref. [33] we obtain a VRI region with the special case of no singular NT. In the special situation of the VRI point of this PES (8) with parameter c=1, the usual criteria for a VRI point, Eqs. (4) for NTs and (6) for GEs do not work appropriately. In contrast, a GE only crosses a Det(**H**)=0-line. This point we can accentuate for a VRI point of type G. One eigenvalue of the Hessian is zero, but the corresponding eigenvector is the gradient. Thus it holds

$$\mathbf{H}\,\mathbf{g} = \mathbf{0}\ . \tag{11}$$

The nature of the PES of this exceptional case is that the one bifurcating valley is a 'dead' valley with no further stationary points.

Appendix 1: Proof of the Index Theorem

We follow references [68, 92, 93]. The Branin Eq. (2) is the desingularized continuous Newton equation. For the minus sign, it converges to a stationary point with an even index, i.e., a minimum with index zero as in the Newton-Raphson method. For plus sign, however, it converges to a stationary point with an odd index, compare Figs.2

and 4 B. It can be developed with a Taylor approach for the gradient

$$\mathbf{g}(\mathbf{x}) \approx \mathbf{g}(\mathbf{x_0}) + \frac{\partial \mathbf{g}}{\partial \mathbf{x}}(\mathbf{x_0})\ (\mathbf{x} - \mathbf{x_0})$$

and for zero gradient at $\mathbf{x_0}$ it is

$$= \mathbf{H}(\mathbf{x_0})\ (\mathbf{x} - \mathbf{x_0})\ .$$

Eq.(2) looks then

$$\frac{d\mathbf{x}}{dt} \approx -\mathbf{A}(\mathbf{x})\mathbf{H}(\mathbf{x_0})\,(\mathbf{x} - \mathbf{x_0})\ \approx -\mathbf{Det}(\mathbf{H}(\mathbf{x_0}))\,(\mathbf{x} - \mathbf{x_0})\ ,$$

and this is attractive for even index, but repulsive for odd index of $\mathbf{H}(\mathbf{x_0})$.

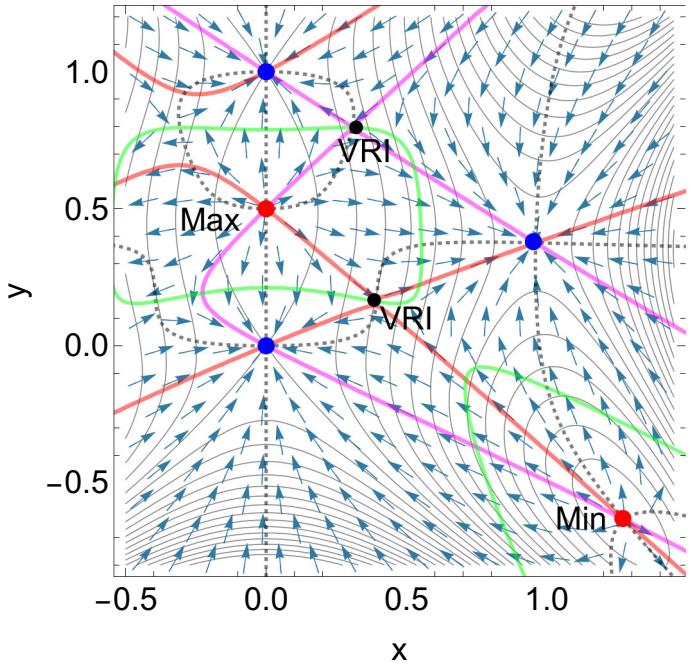

Fig. 8 PES (8) with c=2 now with an SP of index two, a maximum. Red points are stationary points with even indices, the minimum and the maximum, while blue points are three SPs of index one, three TSs. Two singular NTs cross two VRI points (black), one NT is red colored, and one NT is in magenta.

For illustration, Fig.8 shows a test surface with three types of stationary points. Regular NTs from the maximum at $(0, 0.5)$ only lead to SPs of index one, and so on. Thus starting near of one of the two kinds of stationary points, an NT (with corresponding $\pm$ change) will lead to the other kind, by an index difference of one. This rule can only be violated by a VRI point on a singular NT.

Appendix 2: Representation of NTs and of GEs

2D PES with NTs [68]
In 2D toy examples, NTs can easily be represented by a graphical rule. It applies in two dimensions that the orthogonal direction to the force direction

$$\mathbf{f}=\binom{f_1}{f_2} \text{ is unique the direction } \mathbf{f}^{\perp} = (-f_2, f_1) \ .$$

Then condition (1) that $\mathbf{f} \,||\, \mathbf{g}$ is the zero of the scalar product

$$\mathbf{f}^{\perp}\ \mathbf{g}\ = \mathbf{0} \ .$$

In Mathematica, one can represent the corresponding NT by
ContourPlot[-g$_1$[x,y] f$_2$[x,y] + g$_2$[x,y] f$_1$[x,y],{x,-2,2},{y,-2,2}, ContourShading→False, Contours→{0.0}]

2D PES with GEs
In analogy to NTs, also GEs can easily be represented by a graphical rule in 2D examples. It applies in two dimensions that the orthogonal direction to the gradient direction

$$\mathbf{g}=\binom{g_1}{g_2} \text{ is unique the direction } \mathbf{g}^{\perp} = (-g_2, g_1) \ .$$

Then condition (5) means that $\mathbf{H}\,\mathbf{g}||\,\mathbf{g}$, and this is again the zero of the scalar product

$$\mathbf{g}^{\perp}\ \mathbf{H}\,\mathbf{g}\ = \mathbf{0} \ .$$

One can display the corresponding GE in a graphic program analogously to above.

Conflict of Interest: We declare that we have no affiliation with or involvement in any organization that has a financial interest in the subject matter or materials discussed herein.

Author Contributions: WQ, HHGCh and JMB contributed equally.

Methods: We have used Mathematica 13.3.1.0 for Linux x86(64-bit) in the calculations and in the representation of the figures.

Data Access Statement: All relevant data are included in the paper. Further data can be obtained from WQ.

Acknowledgements: JMB thanks the Spanish Structures of Excellence María de Maeztu Program, Grant CEX2021-001202-M, and the Agència de Gestió d'Ajuts Universitaris i de Recerca of Generalitat de Catalunya, Projecte 2021 SGR 00354.
GHHCh acknowledges support from the Max-Planck Gesellschaft via the MPI-PKS visitors program.

References

[1] Stewart, I.: Applications of catastrophe theory to the physical sciences. Physica D **2**, 245–305 (1981)

[2] Crawford, J.D.: Introduction to bifurcation theory. Rev. Mod. Phys. **63**, 991–1037 (1991)

[3] Valtazanos, P., Ruedenberg, K.: Bifurcations and transition states. Theor. Chim. Acta **69**, 281–307 (1986)

[4] Baker, J., Gill, P.M.W.: An algorithm for the location of branching points on reaction paths. J. Comput. Chem. **9**, 465–475 (1988)

[5] Yamamoto, N., Bernardi, F., Bottoni, A., Olivucci, M., Robb, M.A., Wilsey, S.: Mechanism of carbene formation from the excited states of diazirine and diazomethane: An MC-SCF study. J. Am. Chem. Soc. **116**, 2064–2074 (1994)

[6] Quapp, W., Hirsch, M., Heidrich, D.: Bifurcation of reaction pathways: the set of valley ridge inflection points of a simple three-dimensional potential energy surface. Theor. Chem. Acc. **100**(5/6), 285–299 (1998)

[7] Margalef-Roig, J., Miret-Artes, S., Toro-Labbe, A.: Characterization of elementary chemical reactions from bifurcation theory. J. Phys. Chem. A **104**, 11589–11592 (2000)

[8] Quapp, W., Hirsch, M., Heidrich, D.: An approach to reaction path branching using valley-ridge inflection points of potential energy surfaces. Theor. Chem. Acc. **112**, 40–51 (2004)

[9] Suhrada, C.P., Selcuki, S., Nendel, N., Cannizzaro, C., Houk, K.N., Rissing, P.-J., Baumann, D., Hasselmann, D.: Dynamic effects on [3,3] and [1,3] shifts of 6-methylenebicyclo[3.2.0]hept-2-ene. Angew. Chem., Int. Ed. **44**, 3548–3552 (2005)

[10] Goldsmith, B.R., Sanderson, E.D., Bean, D., Peters, B.: Isolated catalyst sites on amorphous supports: A systematic algorithm for understanding heterogeneities in structure and reactivity. J. Chem. Phys. **138**, 204105 (2013)

[11] Windhorn, L., Yeston, J.S., Witte, T., Fuss, W., Motzkus, M., Proch, D., Kompa, K.L., Moore, C.B.: Getting ahead of IVR: A demonstration of mid-infrared induced molecular dissociation on a sub-statistical time scale. J. Chem. Phys. **119**, 641–644 (2003)

[12] Michel, L.: Symmetry defects and broken symmetry. Configurations. Hidden symmetry. Rev. Mod. Phys. **52**, 617–651 (1980)

[13] Kraus, W.A., DePristo, A.E.: Reaction dynamics on bifurcating potential energy surfaces. Theoret. Chim. Acta **69**, 309–322 (1986)

[14] Bakken, V., Danovich, D., Shaik, S., Schlegel, H.B.: A single transition state serves two mechanisms: An ab initio classical trajectory study of the electron transfer and substitution mechanisms in reactions of ketyl radical anions with alkyl halides. J. Am. Chem. Soc. **123**, 130–134 (2001)

[15] Limanto, J., Khuong, K.S., Houk, K.N., Snapper, M.L.: Intramolecular cycloadditions of Cyclobutadiene with Dienes: Experimental and computational studies of the competing $(2+2)$ and $(4+2)$ modes of reaction. J. Am. Chem. Soc. **125**, 16310–16321 (2003)

[16] Lasorne, B., Dive, G., Lauvergnat, D., Desouter-Lecomte, M.: Wave packet dynamics along bifurcating reaction paths. J. Chem. Phys. **118**(13), 5831–5840 (2003)

[17] Zheng, J., Papajak, E., Truhlar, D.G.: Phase space prediction of product branching ratios: Canonical competitive nonstatistical model. J. Am. Chem. Soc. **131**(43), 15754–15760 (2009)

[18] Rehbein, J., Carpenter, B.K.: Do we fully understand what controls chemical selectivity? Phys. Chem. Chem. Phys. **13**, 20906–20922 (2011)

[19] Ohashi, M., Liu, F., Hai, Y., Chen, M., Tang, M.-c., Yang, Z., Sato, M., Watanabe, K., Houk, K.N., Tang, Y.: SAM-dependent enzyme-catalysed pericyclic reactions in natural product biosynthesis. Nature **549**, 502–506 (2017)

[20] Ge, L., Li, S., George, T.F., Sun, X.: A model of intrinsic symmetry breaking. Phys. Lett. A **377**, 2069–2073 (2013)

[21] Sanchez-Galvez, A., Hunt, P., Robb, M.A., Olivucci, M., Vreven, T., Schlegel, H.B.: Ultrafast radiationless deactivation of organic dyes: evidence for a two-state two-mode pathway in polymethine cyanines. J. A. Chem. Soc. **122**, 2911–2924 (2000)

[22] Wang, Z., Hirschi, J.S., Singleton, D.A.: Recrossing and dynamic matching effects on selectivity in a Diels-Alder reaction. Angew. Chem. Int. Ed Engl. **48**(48), 9156–9159 (2009)

[23] Chuang, H.-H., Tantillo, D.J., Hsu, C.-P.: Construction of two-dimensional potential energy surfaces of reactions with post-transition-state bifurcations. J. Chem. Theory Computat. **16**(7), 4050–4060 (2020)

[24] Çelebi-Ölçüm, N., Ess, D.H., Aviyente, V., Houk, K.N.: Lewis acid catalysis alters the shapes and products of bis-pericyclic Diels-Alder transition states. J. Am. Chem. Soc. **129**, 4528–4529 (2007)

[25] Ess, D.H., Wheeler, S.E., Iafe, R.G., Xu, L., Çelebi-Ölçüm, N., Houk, K.N.: Bifurcations on potential energy surfaces of organic reactions. Angew. Chem. Int. Ed.

47, 7592–7601 (2008)

[26] Lee, S., Goodman, J.M.: Rapid route-finding for bifurcating organic reactions. J. Am. Chem. Soc. **142**(20), 9210–9219 (2020)

[27] Katsanikas, M., Garcia-Garrido, V.J., Agaoglou, M., Wiggins, S.: Phase space analysis of the dynamics on a potential energy surface with an entrance channel and two potential wells. Phys. Rev. E **102**, 012215 (2020)

[28] Crossley, R., Agaoglou, M., Katsanikas, M., Wiggins, S.: From Poincaré maps to Lagrangian descriptors: The case of the valley ridge inflection point potential. Regul. Chaot. Dyn. **26**, 147–164 (2021)

[29] Fukui, K.: A formulation of the reaction coordinate. J. Phys. Chem. **74**, 4161–4163 (1970)

[30] Quapp, W., Heidrich, D.: Analysis of the concept of minimum energy path on the potential energy surface of chemically reacting systems. Theor. Chim. Acta **66**, 245–260 (1984)

[31] Taketsugu, T., Yanai, T., Hirao, K., Gordon, M.S.: Dynamic reaction path study of SiH4+F- → SiH4F- and the Berry pseudorotation with valley-ridge inflection. J. Molec. Struc.: THEOCHEM **451**(1-2), 163–177 (1998)

[32] Maeda, S., Harabuchi, Y., Ono, Y., Taketsugu, T., Morokuma, K.: Intrinsic reaction coordinate: Calculation, bifurcation, and automated search. Int. J. Quant. Chem. **115**, 258–269 (2015)

[33] Su, H., Wang, H., Zhang, L., Zhao, J., Zheng, X.: Improved high-index saddle dynamics for finding saddle points and solution landscape. arXiv **2502.03694v2**, 1–19 (2025)

[34] Quapp, W., Bofill, J.M.: A contribution to a theory of mechanochemical pathways by means of Newton trajectories. Theoret. Chem. Acc. **135**(4), 113 (2016)

[35] Quapp, W., Bofill, J.M.: Towards a theory of mechanochemistry- simple models from the very beginning. Int. J. Quant. Chem. **118**, 5775 (2018)

[36] Quapp, W., Bofill, J.M.: Theory and examples of catch bonds. J. Phys. Chem. B **128**(17), 4097–4110 (2024)

[37] Branin, F.H.: Widely convergent methods for finding multiple solutions of simultaneous nonlinear equations. IBM J. Res. Develop. **16**, 504–522 (1972)

[38] Jongen, H.T., Jonker, P., Twilt, F.: Nonlinear Optimization in Finite Dimensions. Kluwer Academic Publ., Dordrecht (2000)

[39] Bofill, J.M.: Updated Hessian matrix and the restricted step method for locating

transition structures. J. Computat. Chem. **15**, 1–11 (1994)

[40] Anglada, J.M., Besalú, E., Bofill, J.M., Rubio, J.: Another way to implement the Powell formula for updating Hessian matrices related to transition structures. J. Math. Chem. **25**, 85–92 (1999)

[41] Hratchian, H.P., Schlegel, H.B.: Using Hessian updating to increase the efficiency of a Hessiian based predictor-corrector relation path following method. J. Chem. Theory Computat. **1**, 61 (2005)

[42] Bofill, J.M., Quapp, W.: Variational nature, integration, and properties of the Newton reaction path. J. Chem. Phys. **134**, 074101 (2011)

[43] Hirsch, M., Quapp, W., Heidrich, D.: The set of valley-ridge inflection points on the potential energy surface of the water molecule. Phys. Chem. Chem. Phys. **1**, 5291–5299 (1999)

[44] Quapp, W., Melnikov, V.: The set of valley ridge inflection points on the potential energy surfaces of H_2S, H_2Se and H_2CO. Phys. Chem. Chem. Phys. **3**, 2735–2741 (2001)

[45] Quapp, W., Hirsch, M., Heidrich, D.: An approch to reaction path branching using valley-ridge-inflection points of potential energy surfaces. Theor. Chem. Acc. **112**, 40–51 (2004)

[46] Bofill, J.M., Quapp, W.: Analysis of the valley-ridge inflection points through the partitioning technique of the Hessian eigenvalue equation. J. Math. Chem. **51**, 1099–1115 (2013)

[47] Quapp, W., Bofill, J.M., Aguilar-Mogas, A.: Exploration of cyclopropyl radical ring opening to allyl radical by Newton trajectories: Importance of valley-ridge inflection points to understand the topography. Theor. Chem. Acc. **129**, 803–821 (2011)

[48] Quapp, W.: Can we understand the branching of reaction valleys for more than two degrees of freedom? J. Math. Chem. **54**, 137–148 (2015)

[49] COLUMBUS: program system. https://columbus-program-system.gitlab.io/columbus/ (2023)

[50] Quapp, W.: Program for unsymmetric valley-ridge inflection points. www.math.uni-leipzig.de/∼quapp/SkewVRIs.html (2011)

[51] Quapp, W.: Mathematica notebook for catch bond calculations. https://community.wolfram.com/groups/-/m/t/3167380 , **Wolfram** (2024)

[52] Quapp, W., Schmidt, B.: An empirical, variational method of approach to unsymmetric valley-ridge inflection points. Theor. Chem. Acc. **128**, 47–61 (2011)

[53] Schmidt, B., Quapp, W.: Search of manifolds of nonsymmetric valley-ridge inflection points on the potential energy surface of HCN. Theor. Chem. Acc. **132**, 1305–1313 (2012)

[54] Garcia-Garrido, V.J., Wiggins, S.: The dynamical significance of valley-ridge inflection points. Chem. Phys. Lett. **781**, 138970 (2021)

[55] Gonzalez, J., Gimenez, X., Bofill, J.M.: A reaction path Hamiltonian defined on a Newton path. J. Chem. Phys. **116**, 8713–8722 (2002)

[56] Quapp, W.: A growing string method for the reaction pathway defined by a Newton trajectory. J. Chem. Phys. **122**, 174106 (2005)

[57] Konda, S.S.M., Brantley, J.M., Bielawski, C.W., Makarov, D.E.: Chemical reactions modulated by mechanical stress: Extended Bell theory. J. Chem. Phys. **135**, 164103 (2011)

[58] Cardozo, T.M., Galliez, A.P., Borges Jr, I., Plasser, F., Aquino, A.J.A., Barbatti, M., Lischka, H.: Dynamics of benzene excimer formation from the parallel-displaced dimer. Phys. Chem. Chem. Phys. **21**, 13916–13924 (2019)

[59] Barkan, C.O., Bruinsma, R.F.: Topology of molecular deformations induces triphasic catch bonding in selectin-ligand bonds. Proc. Natl. Acad. Sci. **121**, 2315866121 (2024)

[60] Hopper, N., Rana, R., Sidoroff, F., Cayer-Barrioz, J., Mazuyer, D., Tysoe, W.T.: Activation volumes in tribochemistry; what do they mean and how to calculate them? Tribol. Lett. **73**, 40 (2025)

[61] Quapp, W.: Finding the transition state without initial guess: the growing string method for Newton trajectory to isomerisation and enantiomerisation reaction of alanine dipeptide and poly(15)alanine. J. Computat. Chem **28**, 1834–1847 (2007)

[62] Hoffmann, D.K., Nord, R.S., Ruedenberg, K.: Gradient extremals. Theor. Chim. Acta **69**, 265–280 (1986)

[63] Sun, J.-Q., Ruedenberg, K.: Gradient extremals and steepest descent lines on potential energy surfaces. J. Chem. Phys. **98**, 9707–9714 (1993)

[64] Quapp, W.: Gradient Extremals and Valley Floor Bifurcation on Potential Energy Surfaces. Theoret. Chim. Acta **75**, 447–460 (1989)

[65] Schlegel, H.B.: Following gradient extremal paths. Theor. Chim. Acta **83**, 15–20 (1992)

[66] Hirsch, M., Quapp, W.: Reaction pathways and convexity of the potential energy surface: Application of Newton trajectories. J. Math. Chem. **36**, 307–340 (2004)

[67] Bofill, J.M., Quapp, W., Caballero, M.: The variational structure of gradient extremals. J. Chem. Theory Computat. **8**, 927–935 (2012)

[68] Hirsch, M.: Zum Reaktionswegcharakter von Newtontrajektorien (in german). Dissertation, University Leipzig, Faculty of Chemistry and Mineralogy (2004)

[69] Quapp, W., J.M.Bofill: Mechanochemistry on the Müller-Brown surface by Newton trajectories. Int. J. Quant. Chem. **118**, 25522 (2018)

[70] Hirsch, M., Quapp, W.: Reaction Channels of the Potential Energy Surface: Application of Newton Trajectories. J. Molec. Struct., THEOCHEM **683**(1-3), 1–13 (2004)

[71] Pechukas, P.: On simple saddle points of a potential surface, the conservation of nuclear symmetry along paths of steepest descent, and the symmetry of transition states. J. Chem. Phys. **64**, 1516–1521 (1976)

[72] Bone, R.G.A.: Deducing the symmetry operations generated at the transition state. Chem. Phys. Lett. **193**, 557–564 (1992)

[73] Schaad, L.J., Hu, J.: Symmetry rules for transition structures in degenerate reactions. J. Am. Chem. Soc. **120**, 1571–1580 (1998)

[74] Minyaev, R.M., Wales, D.J.: Gradient line reaction path of HF addition to ethylene. Chem. Phys. Lett. **218**(5-6), 413–421 (1994)

[75] Harabuchi, Y., Taketsugu, T.: A significant role of the totally-symmetric valley-ridge inflection point in the bifurcating reaction pathway. Theoret. Chem. Acc. **130**, 305–315 (2011)

[76] Zhou, C., Birney, D.M.: Sequential transition states and the valley-ridge inflection point in the formation of a semibullvalene. Organic Lett. **4**, 3279–3282 (2002)

[77] Debbert, S.L., Carpenter, B.K., Hrovat, D.A., Borden, W.T.: The iconoclastic dynamics of the 1,2,6-heptatriene rearrangement. J. Am. Chem. Soc. **124**, 7896–7897 (2002)

[78] Pomerantz, A., Camden, J.P., Chioiu, A.S., Ausfelder, F., Chawia, N., Hase, W.L., Zare, R.N.: Reaction products with internal energy beyond the kinematic limit result from trajectories far from the minimum energy path: An example from H+HBr $\rightarrow$ H_2 + Br. J. Am. Chem. Soc. **127**(47), 16368–16369 (2005)

[79] Okada, K., Sugimoto, M., Saito, K.: A reaction-path dynamics approach to the thermal unimolecular decomposition of acetaldoxime. Chem. Phys. **189**, 629–636 (1994)

[80] Shustov, G.V., Rauk, A.: Mechanism of dioxirane oxidation of CH bonds, application to homo- and heterosubstituted alkanes as a model of the oxidation of

peptides. J. Organic Chem. **63**(16), 5413–5422 (1998)

[81] Carpenter, B.K., Harvey, J., Glowacki, D.: Prediction of enhanced solvent-induced enantioselectivity for a ring opening with a bifurcating reaction path. Phys. Chem. Chem. Phys. **17**, 8372–8381 (2015)

[82] Mann, D.J., Hase, W.L.: Ab initio direct dynamics study of cyclopropyl radical ring-opening. J. Am. Chem. Soc. **124**, 3208–3209 (2002)

[83] Taketsugu, T., Kumeda, Y.: An ab initio direct-trajectory study of the kinetic isotope effect on the bifurcating reaction. J. Chem. Phys. **114**, 6973–6982 (2001)

[84] Gonzalez-Lafont, A., Moreno, M., Lluch, J.M.: Variational transition state theory as a tool to determine kinetic selectivity in reactions involving a valley-ridge inflection point. J. Am. Chem. Soc. **126**, 13089–13094 (2004)

[85] Ussing, B.R., Hang, C., Singleton, D.A.: Dynamic effects on the periselectivity, rate, isotope effects, and mechanism of cycloadditions of ketenes with cyclopentadiene. J. Am. Chem. Soc. **128**, 7594–7607 (2006)

[86] Thomas, J.B., Waas, J.R., Harmata, M., Singleton, D.A.: Control elements in dynamically determined selectivity on a bifurcating surface. J. Am. Chem. Soc. **130**, 14544–14555 (2008)

[87] Yamamoto, Y., Hasegawa, H., Yamataka, H.: Dynamic path bifurcation in the Beckmann reaction: Support from kinetic analyses. J. Org. Chem. **76**, 4652–4660 (2011)

[88] Hong, Y.J., Tantillo, D.J.: Biosynthetic consequences of multiple sequential post-transition-state bifurcations. Nat. Chem. **6**, 104–111 (2014)

[89] Kong, W.-Y., Hu, Y., Guo, W., Potluri, A., Schomaker, J.M., Tantillo, D.J.: Synthetically relevant post-transition state bifurcation leading to diradical and zwitterionic intermediates: Controlling nonstatistical kinetic selectivity through solvent effects. J. Am. Chem. Soc. (2025)

[90] Boltzmann, L.: Vorlesungen über Gastheorie. J. A. Barth, Leipzig (1898)

[91] Müller, K., Brown, L.D.: Location of saddle points and minimum energy paths by a constrained simplex optimisation procedure. Theor. Chim. Acta **53**, 75–93 (1979)

[92] Diener, I.: Globale Aspekte des kontinuierlichen Newtonverfahrens. Habilitation, University Göttingen, Göttingen (1991)

[93] Diener, I.: Trajectory methods in global optimization. In: Horst, R., Pardalos, P.M. (eds.) Handbook of Global Optimization. Nonconvex Optimization and Its Applications, vol. 2, pp. 649–668. Springer, US (1995)